BIOCHEMISTRY
including biophysical chemistry & molecular biology

Article

pubs.acs.org/biochemistry

Phosphorylation Controls the Interaction of the Connexin43 C-Terminal Domain with Tubulin and Microtubules

Amal Saidi Brikci-Nigassa,[†,§] Marie-Jeanne Clement,[†] Tap Ha-Duong,[‡] Elisabeth Adjadj,[†] Latifa Ziani,[†] David Pastre,[†] Patrick A. Curmi,*[,†] and Philippe Savarin*[,†]

[†]Institut National de la Santé et de la Recherche Médicale (INSERM), UMR829, Université Evry-Val d'Essonne, Laboratoire Structure-Activité des Biomolécules Normales et Pathologiques, Evry 91025, France

[‡]Centre National de la Recherche Scientifique (CNRS), UMR 8587, Université Evry-Val d'Essonne, Laboratoire Analyse et Modélisation pour la Biologie et l'Environnement, Evry 91025, France

Supporting Information

ABSTRACT: Connexins are structurally related transmembrane proteins that assemble to form gap junction channels involved in the mediation of intercellular communication. It has been shown that the intracellular tail of connexin43 (Cx43) interacts with tubulin and microtubules with putative impacts on its own intracellular trafficking, its activity in channel communication, and its interference with specific growth factor signal transduction cascades. We demonstrate here that the microtubule binding of Cx43 is mainly driven by a short region of 26 amino acid residues located within the intracellular tail of Cx43. The nuclear magnetic resonance structural analysis of a peptide (K26D) corresponding to this region shows that this peptide is unstructured when free in solution and adopts a helix conformation upon binding with tubulin. In addition, the resulting K26D−tubulin molecular complex defines a new structural organization that could be shared by other microtubule partners. Interestingly, the K26D−tubulin interaction is prevented by the phosphorylation of K26D at a src kinase specific site. Altogether, the results elucidate the mechanism of the interaction of Cx43 with the microtubule cytoskeleton and propose a pathway for understanding the microtubule-dependent regulation of Cx43 gap junctional communications and the involvement of Cx43 in TGF-β signal transduction.

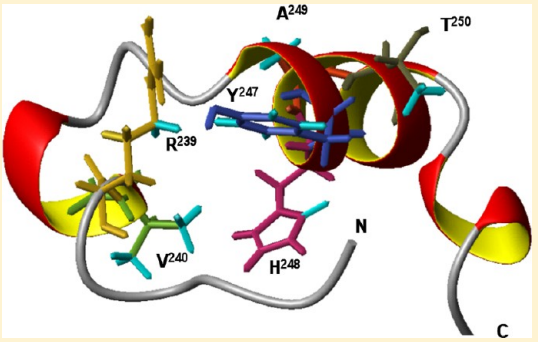

Connexins are transmembrane proteins that form hexameric hemichannels (connexons). The docking of two connexons from neighboring cells leads to the formation of a gap junction channel that allows the rapid passage of ions and small metabolites (<1000 Da) between adjacent cells. These channels participate in paracrine signaling under different conditions such as cell proliferation or differentiation, electrical coupling, embryonic development, and tissue homeostasis.[1−4]

The connexin family consists of 21 isoforms in humans,[5] named according to their predicted molecular masses in kilodaltons (e.g., 43 kDa connexin is named connexin43 or Cx43).[6] At the molecular level, connexins organize as tetraspan membrane proteins with two extracellular loops and three intracellular regions represented by the N- and C-terminal domains and the loop linking transmembrane domains 2 and 3.[3,7] Connexin isoforms present a high level of homology except for the intracytoplasmic loop and C-terminal domain.[3,8]

Cx43 is the most abundant and best studied member of this family. The C-terminal domain of Cx43 (Cx43CT) may interact with various protein partners, including tight junction components such as Zonula occludens-1 (ZO-1), molecules involved in adherens junction as cadherins, α- and β-catenin,[9,10] kinases and phosphatases that regulate the assembly or function of Cx43, and finally components of the cytoskeleton like actin, actin-binding proteins (α-spectrin and drebrin), and microtubules (MTs).[11] With regard to microtubules, experimental data have shown that the Cx43CT fragment of residues 228−260[a] interacts directly with tubulin and microtubules.[12,13] Such an interaction is of interest in at least three different contexts: (i) the intracellular trafficking of Cx43 (it was found that the forward traffic of Cx43 occurs in part along MTs),[14−18] (ii) the functional regulation of gap junction channels (phosphorylation of Cx43CT can modulate gap junction permeability),[19−24] and (iii) the regulation of TGF-β signaling (Smads are transcription factors involved in TGF-β signaling). Among them, non-phosphorylated Smad2 and -3 can bind to tubulin through their MH2 domain and be sequestered on the microtubule surface. It has been proposed that Cx43 and Smads compete for microtubule binding,[13] which may provide a Cx43-dependent mechanism for regulating the TGF-β pathway in relation to cell-to-cell communication.[13,25,26]

To date, no data about the structure of Cx43CT are available to document its interaction with tubulin and MTs. We thus investigated here for the first time by nuclear magnetic

Received: December 8, 2011
Revised: April 9, 2012
Published: May 4, 2012

resonance (NMR) spectroscopy the structural determinants of this interaction through the analysis of the conformational properties of a peptide (K26D, amino acid residues 234−259) derived from the Cx43CT region recognized as being necessary and sufficient for binding to tubulin and MTs. Our results demonstrate that the K26D peptide interacts directly and specifically with tubulin and microtubules and adopts upon binding a compact helical structure. Interestingly, we discovered that K26D−tubulin or −MT binding is negatively regulated by phosphorylation of the K26D tyrosine residue Y247, which is a target for Src kinase. Finally, in attempt to improve our understanding of the competition between Smad2 and Cx43 on tubulin, we succeeded in identifying a tubulin-binding area of the MH2 domain of Smad2.

MATERIALS AND METHODS

Tubulin Purification. Tubulin was purified from sheep brain crude extracts as described previously.[27] Pure tubulin was stored at −80 °C in 50 mM MES-KOH (pH 6.8), 0.5 mM EGTA, 0.25 mM $MgCl_2$, 0.5 mM EDTA, 0.1 mM GTP, and 33% glycerol (v/v). Before use, an additional cycle of assembly and disassembly was performed to remove nonfunctional tubulin. The concentration of tubulin was measured by ultraviolet spectrophotometry at 278 nm using an extinction coefficient of 1.2 mg^{-1} cm^2.[28]

Peptide Synthesis. The K26D, K26D-P (a K26D variant in which Y247 was phosphorylated), and M19T peptides were purchased from PolyPeptide Laboratories (Strasbourg, France). The purity and integrity of the peptides were verified by mass spectrometry. Peptides were dissolved in water at a concentration of 4 mM for stock solutions.

Peptide−Microtubule Cosedimentation Assays. Tubulin (20 μM) was assembled in paclitaxel polymerization buffer [50 mM MES-KOH (pH 6.8), 4 mM $MgCl_2$, 100 mM KCl, 1 mM GTP, 10% glycerol, and 20 μM paclitaxel] for 30 min at 37 °C in the absence or presence of 600 μM K26D peptide. After polymerization, microtubules were pelleted by centrifugation (25000*g* for 15 min at 37 °C) to separate microtubules and the supernatant that contains soluble molecules. Supernatants and resuspended pellets [resuspended in a volume of one-dimensional (1D) sodium dodecyl sulfate−polyacrylamide gel electrophoresis (SDS−PAGE) sample buffer equal to that of the supernatants] were analyzed by SDS−PAGE to determine the amounts of tubulin and peptides in the microtubule and supernatant fractions.

NMR Spectroscopy. NMR spectra were recorded at 9 and 20 °C on a Bruker Avance 600 MHz NMR spectrometer equipped with a cryoprobe. Data were processed using Topspin 2.1 (Bruker) and analyzed using NMRVIEW version 5.2.[29] In all experiments, suppression of the water signal was achieved with the ES[30] or the WATERGATE sequence[31] before acquisition. All NMR samples were prepared in 50 mM deuterated PIPES (pH 6.4) [piperazine-1,4-bis(2-ethanesulfonic acid)]. 2,2-Dimethyl-2-silapentane-5-sulfonate (DSS) was used as an external reference for proton chemical shifts.

^{1}H resonance assignments were determined for free peptides (K26D, K26D-P, or M19T) at a concentration of 800 μM using the standard procedures[32] based on the identification of spin systems using TOCSY spectra[33] and sequential assignments using NOESY spectra[34] with mixing times of 80 and 200 ms respectively. The complete resonance assignments of the K26D, K26D-P, and M19T peptides are given in Tables S1−S3 of the Supporting Information respectively.

The two-dimensional transferred nuclear Overhauser spectroscopy (tr-NOESY)[35,36] experiments with K26D and K26D-P in the presence of tubulin or microtubules were performed at a 20:1 peptide:tubulin molar ratio with two different mixing times (150 and 200 ms). For these experiments, MTs were prepared as described in the preceding section using a tubulin concentration of 40 μM. Control tr-NOESY spectra were recorded in the presence of bovine serum albumin (BSA) in place of tubulin using similar experimental conditions.

One-dimensional saturation transfer difference NMR (STD-NMR)[37] spectra of peptides in the presence of tubulin or MTs were recorded with selective saturation of the resonances of the tubulin methyl group with on-resonance irradiation at −0.5 ppm and off-resonance irradiation at 40 ppm for reference spectra. A series of 40 Gaussian-shaped pulses (50 ms with a 1 ms delay between pulses) were used for a total saturation time of 2.04 s. Control 1D ^{1}H STD-NMR spectra were recorded in the presence of peptide alone using similar experimental conditions to certify that the irradiation at −0.5 ppm does not affect the peptide resonances.

Structure Calculation. The three-dimensional structure of the K26D peptide bound to tubulin was calculated by means of a simulated annealing protocol provided in Crystallography & NMR System version 1.1.[38] Torsion angle and distance constraints were used for the structure calculation. The torsion angle constraints were generated with TALOS based on Hα chemical shifts.[39] The tr-NOE intensities (I) were measured with NMRView[29] and then converted to distances[40] using the relationship $I_{ij}/I_{ref} = (r_{ref}/r_{ij})^6$. The calibration of the nuclear Overhauser effect (NOE) distance constraints was based on the fixed distance between the Hδ and Hε protons of Y247.

Of the 100 calculated structures, the 10 lowest-energy structures were selected for further analyses. The structural quality of these structures was analyzed with PROCHECK NMR version 3.5.4.[41] MOLMOL version 2.6[42] was used to visualize the structures and to identify and visualize hydrogen bonds.

Docking Calculations. Docking models of peptide−tubulin complexes were obtained using the coarse-grained protein−protein potential developed by Basdevant et al.[43] allowing a quasi-exhaustive search of their most probable quaternary structures. This simplified model describes each amino acid backbone with one bead and the side chains with one or two other grains, depending on their size. The effective van der Waals and Coulomb potentials between coarse grains were parametrized from an atomic model that preserves the specificity of protein−protein interactions. Such a molecular modeling method has been shown to efficiently predict the quaternary structure of protein−protein or peptide−protein complexes.[44,45] The docking procedure began with the generation of a set of initial conformations of the complex with quasi-exhaustive different positions and orientations of the peptide relative to tubulin. Each configuration was created so that the intermolecular distance between the closest coarse grains was adjusted to 4 Å. The two latitude and longitude angles that characterized the position and the three Euler angles that describe the orientation were sampled regularly with an incremental angle of 30°. For the analysis of the docked structures, an intergrain distance of 5.0 Å was defined as the upper threshold for filtering the groups considered to be close in space and thus in interaction. For these calculations, the three-dimensional structure of tubulin [Protein Data Bank (PDB) entry 1JFF], in which paclitaxel, zinc, and GTP were

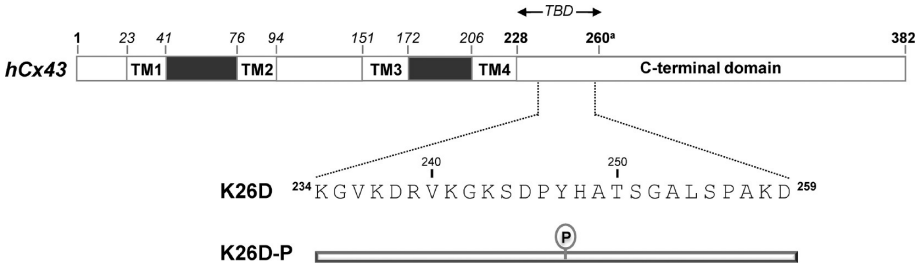

Figure 1. Schematic representation of human connexin43 (hCx43) and of the K26D and K26D-P peptides. The hCx43 sequence possesses four transmembrane (TM) and three cytoplasmic domains. Peptides were derived from the Cx43 tubulin binding domain (TBD) as described in Results. See footnote *a* for residue 260.

not taken into account, was considered as a starting model. Peptide−microtubule complexes were built using a microtubule model kindly provided by K. Downing (Bioenergy/GTL and Structural Biology Department, Lawrence Berkeley National Laboratory, Berkeley, CA). Molecules were visualized with PyMOL.[46]

RESULTS

Cx43CT Interacts Specifically with Tubulin and Microtubules. In their pioneer work, Giepmans et al. pointed out a putative tubulin-binding domain located within the span of amino acid residues 228−260[a] of Cx43 in the juxtamembrane region of its C-terminal tail.[12] To shed light on the structural determinants of this interaction, we designed a peptide extracted from this Cx43 region. As the first six residues of the domain established by Giepmans (LFYVFF) are highly hydrophobic and thus may lead to an artifact peptide oligomerization not compatible with solution structure investigations, the peptide synthesis was started at residue K234. In addition, to prevent the formation of disulfide bridges, the last cysteine residue (C260) of the proposed motif was not considered (Figure 1).

As a preliminary step before structure investigations, we first checked the interaction of the K26D peptide with microtubules using cosedimentation assays (Figure 2). Microtubule samples were prepared as described in Materials and Methods. As expected, more than 95% of the tubulin was found in the microtubule fraction (pellet) (Figure 2, lanes 1 and 2); 600 μM K26D peptide were then mixed with microtubules prepared under the same conditions. The K26D peptide was found in both the microtubule and the supernatant fractions (Figure 2, lanes 3 and 4), while it remained only in the supernatant when centrifuged in the absence of microtubules as a control (Figure 2, lanes 5 and 6). These results indicate that the K26D peptide does interact with microtubules. To complete these preliminary investigations, we also evaluated the impact of K26D on the dynamics of microtubule assembly using standard in vitro assays.[47] We observed that K26D does not change the assembly rate or the microtubule plateau value (Figure S1 of the Supporting Information).

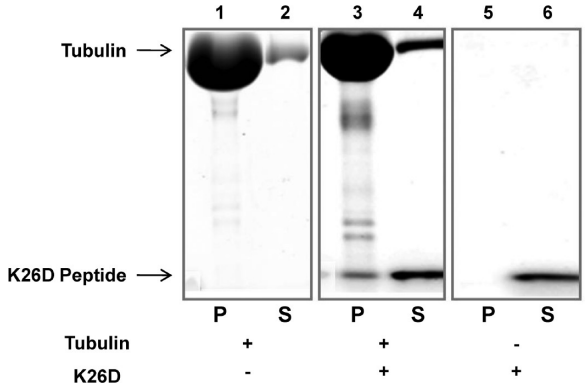

Figure 2. K26D interacts with microtubules. Paclitaxel (20 μM)-stabilized microtubules were centrifuged under control conditions (lanes 1 and 2) or in the presence of 600 μM K26D peptide. In the absence of microtubules, the K26D peptide was found exclusively in the supernatant (S, lane 6) but detected in the pellet (P) when centrifuged in the presence of microtubules (lane 3).

We then initiated a solution NMR structural analysis of the interaction of the K26D peptide with tubulin and microtubules using first STD-NMR spectroscopy. This technique represents a powerful tool for identifying the protons of a small molecule, like a peptide or a protein subdomain, that participate in the interaction with a large protein partner like here tubulin or microtubules.[48−50] STD-NMR experiments allowed us to show that a series of charged (R239, H248, and lysine) and hydrophobic (V240, Y247, and A249) amino acid residues as well as the T250 residue of the K26D peptide interact with tubulin (Figure 3A). Thus, at least two different regions of the peptide seem to be required for the binding: a first region in the N-terminal part comprising residues R239 and V240 and a second one from residue Y247 to T250. Interestingly, similar results were obtained when the STD-NMR experiment was performed using microtubules instead of tubulin (Figure 3B). The specificity of the K26D−tubulin or −MT interaction was ascertained by the absence of significant magnetization transfer when BSA was substituted for tubulin as a control (Figure S2 of the Supporting Information). The solution NMR structure of the peptide bound to tubulin was then investigated to determine the spatial organization of the binding regions involved in the recognition of tubulin or MTs as revealed by the STD-NMR experiments.

The K26D Peptide Is Structured upon Tubulin Binding. We first examined the structure of K26D when free in solution. From structural predictions performed with HHPred,[51] the conformation of K26D appeared mainly as a random coil with a helical tendency between residues 246 and 252. NMR experiments showed that K26D is largely unstructured with, nevertheless, a helical tendency in agreement with structural predictions. Indeed, analysis of the Hα chemical shifts deviations ($\Delta\delta$Hα) of K26D showed that residues 245−248 have negative deviations (less than −0.1 ppm) from their random coil values,[52] indicating the presence of a local α-helix (Figure S3 of the Supporting Information).

dx.doi.org/10.1021/bi201806j | *Biochemistry* 2012, 51, 4331−4342

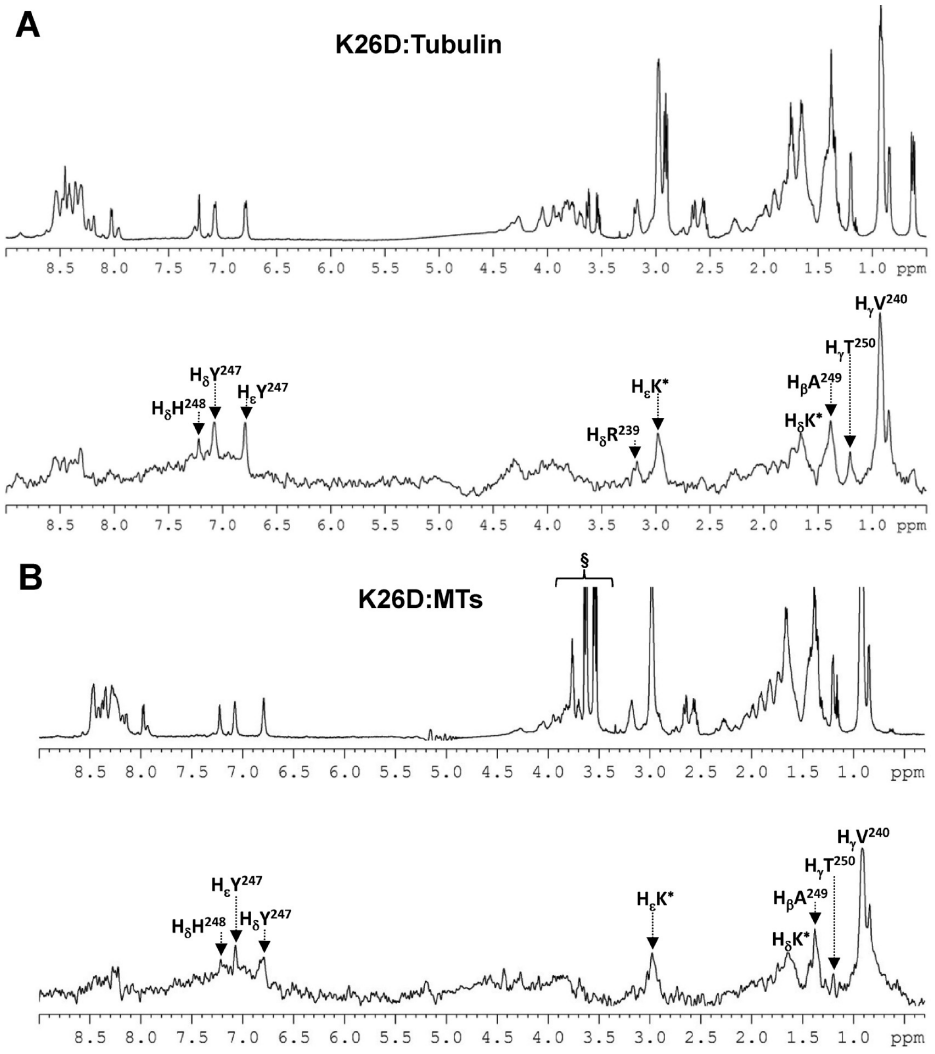

Figure 3. STD-NMR spectroscopy reveals a specific interaction of K26D with tubulin. 1D proton NMR spectrum of 800 μM K26D in the presence of 40 μM tubulin (A, top) or in the presence of paclitaxel-stabilized MTs that were assembled from tubulin at a concentration of 40 μM (B, top) and corresponding STD-NMR spectra showing that the K26D peptide interacts with tubulin through a series of charged and hydrophobic residues (bottom spectra of panels A and B). Protons of K26D residues implicated in the interaction with MTs are denoted. Spectra were recorded in 50 mM deuterated PIPES (pH 6.4) at 20 °C. For STD spectra, tubulin (A) and MTs (B) were selectively saturated by applying a frequency irradiation at −0.5 ppm. Asterisks denote ambiguous assignments. §, MES buffer.

The K26D structure bound to tubulin was then investigated using tr-NOESY experiments. The comparison of the NOESY spectrum of the K26D peptide (Figure 4A) with its tr-NOESY spectrum recorded in the presence of tubulin (Figure 4B) shows a significant reinforcement of some NOEs and an increase in the number of cross-peaks when K26D is in complex with tubulin. The reinforced and additional cross-peaks observed in the presence of tubulin correspond to tr-NOEs that confirm the interaction of the peptide with tubulin. These tr-NOEs contain information about the structural organization of the peptide upon its binding to tubulin. Their analysis showed the presence of intraresidue and sequential interactions but also medium- and long-range interactions [R239(Hβ)−Y247(Hε), V240(Hγ)−Y247(Hδ), V240(Hγ)−H248(Hε), and S251(Hα)−A253(HN)] (Figure 4B) that reflect the folding of the peptide folds in the presence of tubulin. The specificity of the binding and folding of K26D in the presence of tubulin was further demonstrated by the fact that such tr-NOE peaks were absent in a control experiment in which BSA was used in place of tubulin (Figure S4 of the Supporting Information).

The tr-NOEs were thus used to derive distance constraints for the determination of the K26D-bound structure. A total of 425 interproton distances along with 24 torsion-angle constraints predicted with a good score by TALOS[53] were used for the structure calculations. The structure statistics of the 10 lowest-energy conformers, from a total of 100 calculated structures, showed low restraint violations and good stereochemical scores (Table 1). The resulting structures are well-defined from residue V240 to A257, with a backbone root-mean-square deviation (rmsd) of 0.21 Å, whereas the N- and C-terminal regions are defined less accurately (Figure 5A). Approximately 86% of the Φ and Ψ angles are located within the most favored and additional allowed regions of the Ramachandran plot (Table 1).

The average K26D structure (derived from the 10 lowest-energy conformations) presented in Figure 5B shows that the peptide adopts a compact helical structure upon its interaction with tubulin. There are three helical regions: a central α-helical

dx.doi.org/10.1021/bi201806j | *Biochemistry* 2012, 51, 4331−4342

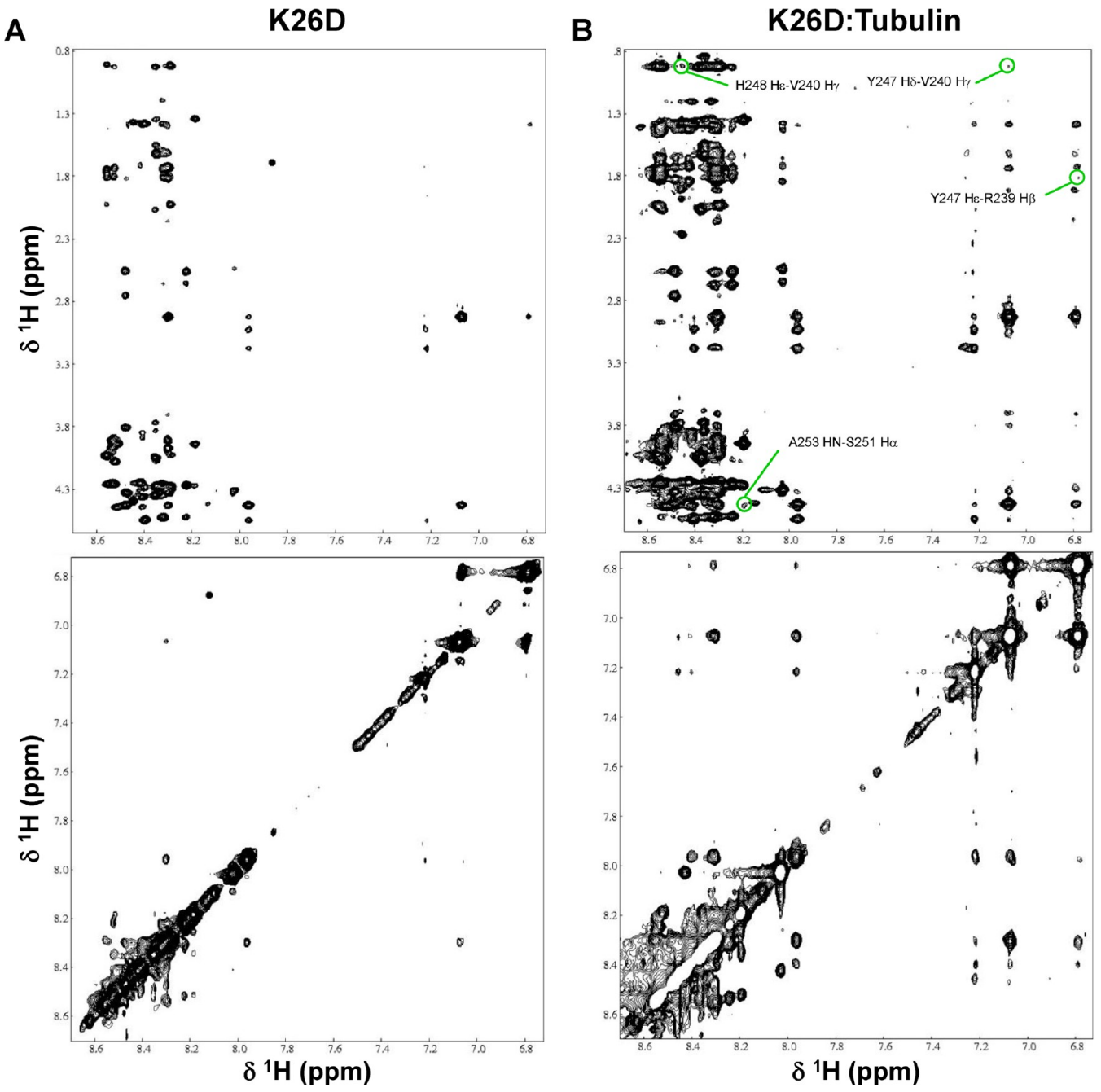

Figure 4. K26D peptide folds upon tubulin binding. (A) Fingerprint (top) and NH−NH (bottom) regions of the NOESY spectrum of 800 μM K26D. (B) tr-NOESY spectrum of the same regions in the presence of 40 μM tubulin. Green circles denote tr-NOEs corresponding to medium- and long-range interactions within the K26D peptide. Spectra were recorded in 50 mM deuterated PIPES (pH 6.4) at 9 °C with a mixing time of 200 ms.

region that spans residues P246−G252 and two 3_{10}-helical regions in the N- and C-termini (V240−G242 and S255−A257). The central α-helical structure is stabilized by hydrogen bonds between Y247(CO) and S251(NH), while the 3_{10}-helical regions are stabilized by hydrogen bonds that connect V240−K243 and L254−A257 for the N- and C-termini, respectively. Finally, we observed that the central and C-terminal helices are joined by a β-turn located between positions G252 (i) and S255 (i + 3). This turn was classified as β-type I on the basis of both the characteristic dihedral angle values (Φ_{i+1} = −57.51 ± 0.31°, Ψ_{i+1} = −24.88 ± 0.89°, Φ_{i+2} = −99.60 ± 1.79°, and Ψ_{i+2} = 7.74 ± 0.5°) and the presence of the hydrogen bond between the CO group of G252(i) and the NH group of S255(i + 3).

The combination of the different structural data obtained for the K26D peptide in interaction with tubulin, shows that the R239−V240 and Y247−T250 stretches from K26D required for tubulin binding according to STD-NMR data correspond to the first two helices observed in the K26D-bound structure. Interestingly, despite the fact that the residues of these two helices are far apart on the K26D primary sequence, their side chains are spatially close within the K26D tubulin-bound structure (Figure 6).

Y247 Phosphorylation of K26D Inhibits Its Binding to Tubulin. The STD-NMR results indicated that residue Y247 of Cx43CT that is present in the K26D peptide is involved in the specific binding of the former to tubulin and MTs. Y247 is

dx.doi.org/10.1021/bi201806j | *Biochemistry* 2012, 51, 4331−4342

Table 1. Structural Statistics of the 10 Best Structures of K26D Bound to Tubulin

number of NMR constraints	
total distance constraints	425
intraresidue	199
sequential ($\|i - j\| = 1$)	152
medium-range ($\|i - j\| \leq 4$)	69
long-range ($\|i - j\| > 4$)	5
number of torsion angle constraints	12 Φ, 12 Ψ
structural statistics	
violation statistics	
number of violations per structure	
NOEs of >0.5 Å	0.60 ± 0.69
dihedral constraint violations of >5°	2.60 ± 1.07
maximal violation NOE (Å)	0.56
maximal torsion angle violation (deg)	8.28
rmsd from ideal geometry	
bond lengths (Å)	0.0119 ± 0.0003
bond angles (deg)	1.14 ± 0.03
improper torsions (deg)	0.82 ± 0.02
Ramachandran plot (%)	
residues in most favored regions	71.1
residues in allowed regions	15.3
residues in generously allowed regions	12.6
residues in disallowed regions	1.1
average rmsd (Å)	
backbone (residues 240−257)	0.21
heavy (residues 240−257)	0.59

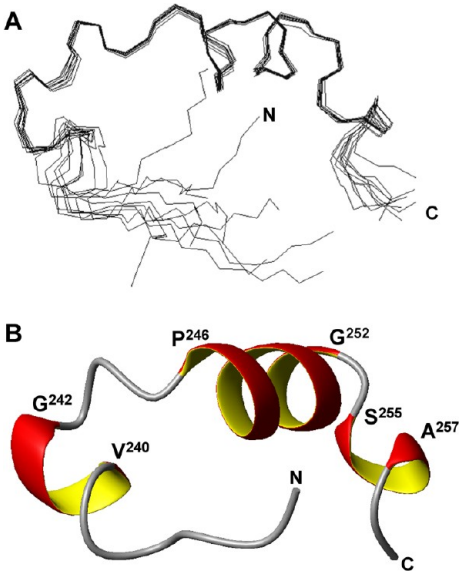

Figure 5. Structure of the tubulin-bound K26D peptide that is compact with short helical regions. (A) Backbone superimposition of the 10 lowest-energy structures of the K26D peptide from residue V240 to A257 (rmsd of 0.21 Å). (B) Ribbon diagram of the mean K26D structure showing three helical regions: a central α-helix and two 3_{10}-helices in the C- and N-terminal regions. This figure was generated with MOLMOL.

known to be phosphorylated by v-Src in the full-length Cx43 protein.[54,55] On the basis of these observations, we postulated that Y247 may represent a putative regulation site for the Cx43−tubulin or −MT interaction. To test this hypothesis, we studied by solution NMR the K26D-P−tubulin interaction. STD-NMR, NOESY, and tr-NOESY spectra were recorded under conditions similar to those used to study the K26D−

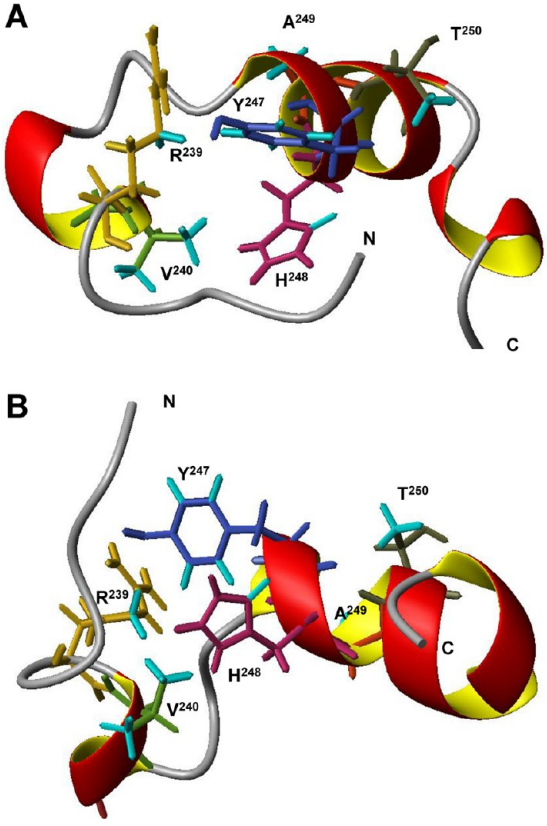

Figure 6. K26D hydrogens involved in tubulin binding are spatially clustered in the K26D-bound structure. Views of the mean K26D structure showing, in cyan, the hydrogens involved in the interaction with tubulin according to STD-NMR results. This figure was generated with MOLMOL.

dx.doi.org/10.1021/bi201806j | *Biochemistry* 2012, 51, 4331−4342

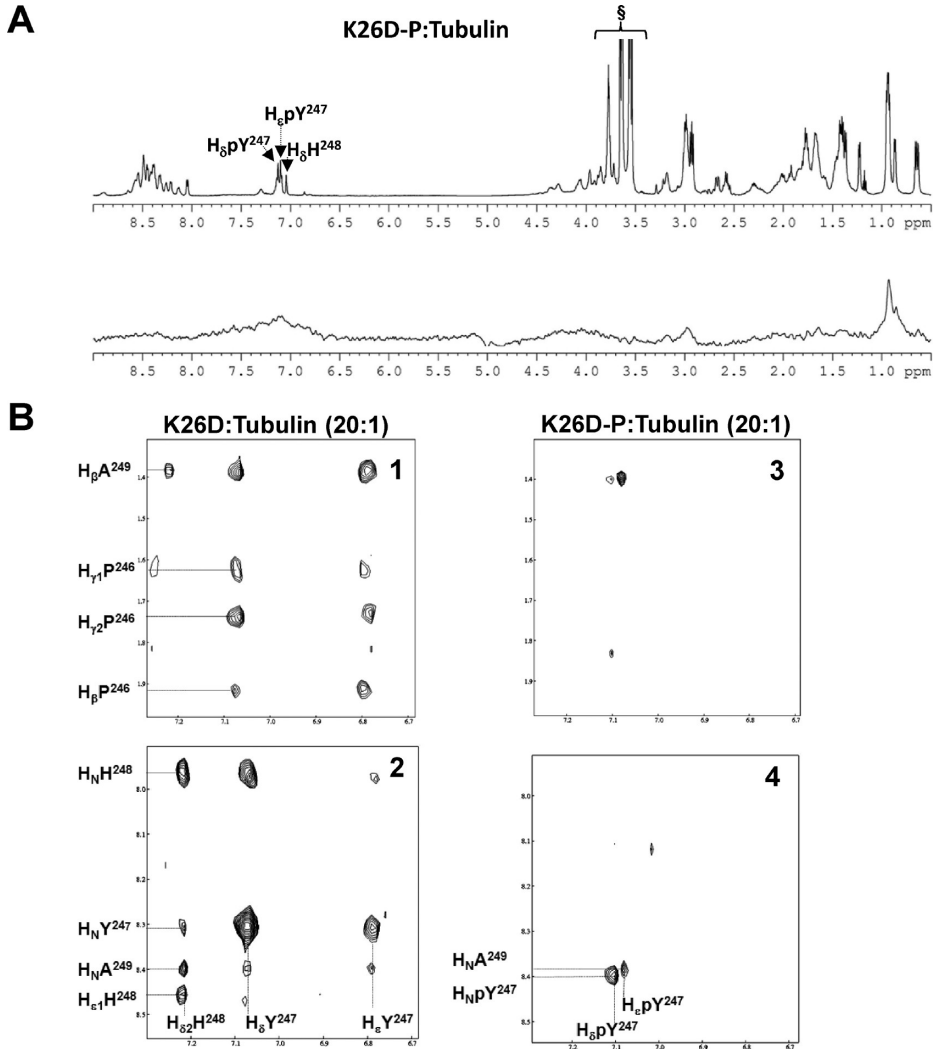

Figure 7. Phosphorylation of Y247 prevents the interaction of K26D with tubulin. (A) 1D proton NMR spectrum of 800 μM K26D-P in the presence of 40 μM tubulin (top) and STD-NMR spectrum showing the absence of specific interaction of the K26D-P peptide with tubulin (bottom). Aromatic protons of Y247 and H_δ of H248 are denoted. (B) tr-NOESY regions of 800 μM K26D (right) and K26D-P (left) in the presence of 40 μM tubulin. Sequential and medium-range NOE cross-peaks involving residues P246, Y247, H248, and A249 observed with K26D disappeared upon Y247 phosphorylation. Spectra were recorded in 50 mM deuterated PIPES (pH 6.4) at 9 °C with a mixing time of 200 ms. §, MES buffer.

tubulin or −MT interaction. The results show that, as for K26D, the K26D-P peptide is not structured when free in solution (data not shown). However, as opposed to K26D, the K26D-P peptide loses its ability to interact with tubulin as demonstrated by the absence of specific K26D proton resonances on the STD-NMR spectra (Figure 7A). In addition, K26D-P does not fold in the presence of tubulin as shown in the tr-NOESY spectrum where the main NOEs related to the tubulin-induced K26D folding are absent (Figure 7B). These data identify Y247 as a critical regulation residue for the interaction of the cytoplasmic tail of Cx43 with the tubulin/MT system.

The Docking of the K26D Peptide on Tubulin Shows Two Different Putative Binding Sites Located on β-Tubulin Only or at the Intradimer $\alpha\beta$-Tubulin Interface. To elucidate the structural organization of the K26D−tubulin complex, molecular modeling calculations were performed using a coarse-grained potential to generate docking models. At a first stage, we calculated three large sets of randomly independent docked models starting with the structure of PDB entry 1JFF of tubulin on one side and the three lowest-energy tubulin-bound K26D NMR conformations that we obtained here on the other. We then selected the five lowest-energy complex models from each of these three large sets. Among the 15 resulting docked structures, seven models were rejected because the grains representing the K26D amino acid residues pointed out by STD-NMR experiments to interact with tubulin were outside the interaction area with tubulin grains. Interestingly, as shown in Figure 8A, the eight remaining docking structures could be divided into three groups of NMR-compatible complex models according to the location of the K26D peptide on tubulin (see the figure legend for model numbering). Within group I, the K26D peptide was found to interact with β-tubulin only, whereas within groups II and III, it is located at the $\alpha\beta$-tubulin intradimer interface next to the tubulin C-terminal tail. Interestingly, tubulin binding zones of groups I and II are compatible with the area identified by Dai and co-workers as a putative Cx43 binding site on tubulin (magenta in the figure). Finally, when the K26D−tubulin complex is transposed to a microtubule model, the K26D peptide appears to dock on the external surface of the

dx.doi.org/10.1021/bi201806j | *Biochemistry* 2012, 51, 4331−4342

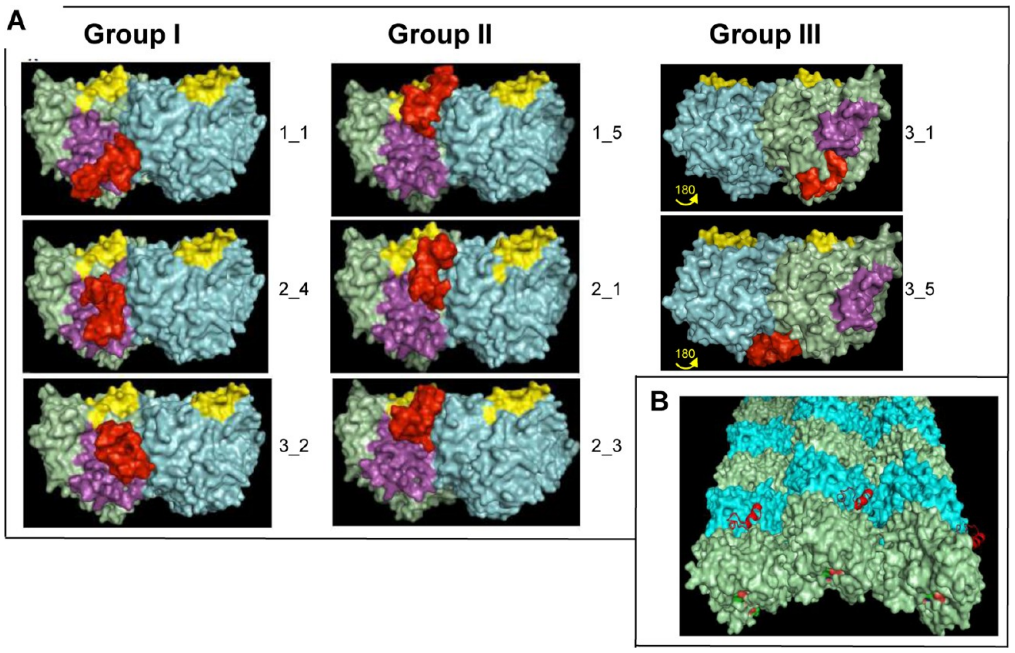

Figure 8. Models of K26D docked on tubulin and microtubule structures. (A) Docking calculations yielded eight K26D−$\alpha\beta$-tubulin models that were compatible with our STD-NMR results. The models are grouped according to the location of the K26D peptide on tubulin. In each group, the model numbering is as follows. The first number corresponds to the K26D NMR structure used for docking calculation. The second number corresponds to the ranking of the model's energy of interaction (1 being used for the lowest interaction energy). In group III models, the orientation of the $\alpha\beta$-tubulin heterodimer has been rotated by 180° to display the docked K26D peptide. Color code: cyan, α-tubulin; green, β-tubulin; yellow, tubulin C-terminal tails (used as a guide for tubulin orientation); red, K26D peptide; magenta, amino acid residues 114−243 of β-tubulin identified by Dai et al.[13] as being critical for Cx43−tubulin interaction. (B) K26D−tubulin complex fit to a microtubule model. The location of the K26D peptide as found in group I or group II models is compatible with docking on the microtubule external surface, whereas K26D from group III appears to dock in the microtubule lumen. The microtubule model was kindly provided by K. Downing. This figure was created with PyMOL.

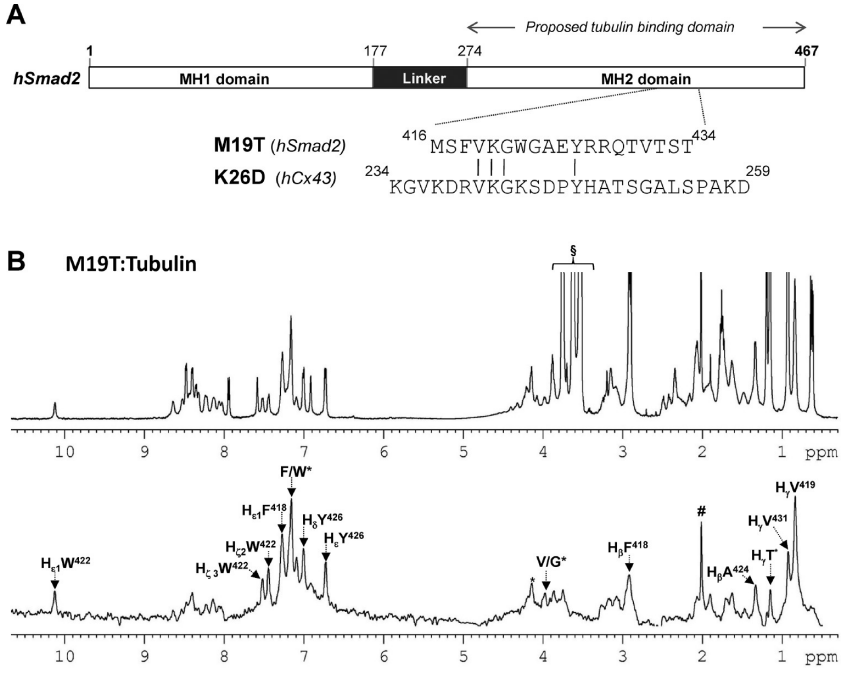

Figure 9. M19T Smad2 peptide interacts with tubulin. (A) Schematic representation of human Smad2 (as designed by Dai et al.) and the derived M19T peptide. The M19T peptide aligns with no gap with the K26D peptide and presents four identical amino acid residues. (B) 1D proton NMR spectrum of 800 μM M19T in the presence of 40 μM tubulin (top) and STD-NMR spectrum of the same sample (bottom). Protons involved in the tubulin binding of M19T are denoted on the spectrum. Asterisks denote ambiguous assignments: T430/T434, V419/G421, and W422/F418. The number sign denotes peptide impurities. §, MES buffer.

microtubule (groups I and II) (Figure 8B) or in the microtubule lumen for group III.

Investigations of the Competition between Smad2 and Cx43 for Tubulin Binding. A series of biochemical and

dx.doi.org/10.1021/bi201806j | *Biochemistry* 2012, 51, 4331−4342

cellular experiments have shown that Cx43 positively regulates the TGF-β pathway by releasing sequestered Smads from microtubules, leading to an increase in the level of phospho-Smad2, the prerequisite for Smad2 hetero-oligomerization, and its activation as a transcription factor.[13] It was proposed that this competition between Cx43 and Smad for tubulin or MT binding may involve the ^{234}KGVKDRVKGK^{243} region of Cx43 (included in the K26D peptide sequence) and the MH2 domain of human Smad2 (amino acids 274−467).[13] To refine the region of Smad2-MH2 responsible for microtubule binding, we made the assumption that such a region should present homologies with the K26D peptide. This led us to propose a 19-amino acid peptide from Smad2-MH2, ranging from M416 to T434 called herein M19T. This selection was based on the following criteria. (i) Four amino acid residues of M19T (V419, K420, G421, and Y426, Smad2 numbering) can be aligned with no gap with the K26D peptide (Figure 9A). (ii) The inspection of the MH2 crystal structure (PDB entry 1KHX)[56] shows that within Smad2, the amino acids corresponding to the M19T peptide are located in a highly solvent-exposed loop (loop L3) and are therefore good candidates for interaction with various partners. (iii) Residues of the L3 loop are predicted to play critical roles in Smad phosphorylation.[56]

The interaction of M19T with tubulin was probed by STD-NMR spectroscopy under conditions similar to those used for the previous peptides. Interestingly, we found that the M19T peptide interacts with tubulin and that, among the four amino acids conserved in the K26D−M19T alignment, two of them (V419 and Y426) are located in the proximity of tubulin (Figure 9B). In addition, other hydrophobic amino acid residues were also identified by the STD-NMR experiments to interact with tubulin: F418, W422, A424, and V431. We next attempted to demonstrate a competition between the K26D and M19T peptides for tubulin binding using STD-NMR experiments. We observed that both peptides can interact simultaneously with tubulin without any influence of one over the other (Figure S5 of the Supporting Information). A tr-NOESY experiment was conducted in the presence of both the M19T and K26D peptides and tubulin. This spectrum revealed the presence of tr-NOEs similar to those observed when the tr-NOESY experiments were performed with a peptide only. Furthermore, no interligand NOEs[57,58] were observed between the K26D and M19T peptides (Figure S6 of the Supporting Information). Altogether, STD-NMR and tr-NOESY experiments suggest that K26D and M19T can interact with tubulin simultaneously on different binding sites.

DISCUSSION

We have addressed here for the first time the structural determinants of the interaction between a peptide from the C-terminal tail of Cx43 and tubulin and microtubules.

When Interacting with Tubulin, the K26D Peptide Folds into a Novel Three-Dimensional (3D) Structure. The K26D peptide binds to tubulin through the minimal ^{239}RVKGKSDPYHAT^{250} sequence with at least two patches of residues (^{239}RV^{240} and ^{247}YHAT^{250}) in the proximity of tubulin. While the K26D peptide is unstructured when free in solution, it folds, when in contact with tubulin or microtubules, in a rather compact 3D conformation containing three different short helices stabilized by hydrogen bonds that leads to a clustering of the tubulin-interacting amino acid residues. It is noteworthy that the structure of K26D possesses an amphiphilic character when bound to tubulin with its hydrophobic residues such as P, Y, and A, located on one side of the α-helix, while the hydrophilic D, H, and S residues are positioned on the other one. This property is probably quite important for the organization of the peptide−tubulin complex. Interestingly, the tubulin-bound K26D fold differs from those reported previously with other tubulin-interacting peptides or proteins[49,59] and suggests the existence of a novel mode of binding to tubulin and microtubules.

Y247 Phosphorylation Regulates the Binding of K26D to Tubulin. It has been reported that the phosphorylation of Cx43 by v-Src at residues Y247 and Y265 disrupts gap junctional communication.[54,60] Among these phosphorylation sites, Y247 appears as the key factor for the Cx43 channel closure.[55] It was suggested that for such closure, the phosphorylation of Cx43 either establishes or disrupts interactions between Cx43 and other protein partners or alters the conformation of Cx43. Our results show that the aromatic ring of Y247 is directly involved in K26D−tubulin binding and that its phosphorylation has a negative impact on tubulin recognition.

K26D May Dock on the Solvent-Exposed Surface of Microtubules or in the Microtubule Lumen. The best docking models of the K26D−tubulin complex were grouped according to their location on tubulin. The K26D peptide appears to interact with β-tubulin only (group I) or at the $\alpha\beta$-tubulin intradimer interface (group II). In both cases, the distances between the K26D peptide and tubulin match our STD-NMR results. Furthermore, the K26D docking sites are clustered in a region of the β-tubulin surface that fully or partially corresponds to that previously underlined by Dai et al. as being the Cx43 binding site on tubulin,[13] so that we cannot favor one group over the other. On the other hand, in group III, the K26D peptide appears outside the region proposed by Dai. When considering the docking of K26D on microtubules, we find the K26D peptide appears at the solvent-exposed surface in both groups I and II, and such docking is displayed for the 3_2 complex in Figure 8B. This location is in agreement with the interaction of Cx43CT with microtubules during its traffic in the cytoplasm toward the cell membrane, and it remains compatible with an interaction of Cx43 with microtubules when Cx43 is localized in gap-junctional plaques. When transposed to microtubules, the group III docking models indicate that K26D may also dock inside the microtubule lumen. Interestingly, this localization may explain the interaction of Cx43 with microtubule extremities at gap-junctional plaques.[12]

Functional Roles of the Cx43 ^{234}K−D^{259} Fragment with Respect to Microtubule Interaction. The most remarkable diversity within the connexin family concerns C-terminal tails that can interact with different protein partners that participate either in the correct formation of functional gap junctions and gap-junction plaques[9,10,61] or with partners that may modulate gene expression.[13] The interaction of Cx43 with microtubules seems to facilitate its intracellular transport,[15] and its recruitment into gap junctions[62] is also critical for cell polarity and cell motility.[63] Microtubules appear also to be necessary for the enhanced assembly of gap junctions as observed in the presence of cholesterol,[15] LDL,[17] or prostaglandines,[64] and they in turn seem to be stabilized by Cx43 at the cell membrane.[12,65] The fact that phosphorylation of the C-terminal tail of Cx43 regulates its interaction with tubulin and MTs opens new perspectives for the regulation of such processes. We further hypothesize that the phosphorylation of the C-terminal tail of Cx43 may occur at the

dx.doi.org/10.1021/bi201806j | Biochemistry 2012, 51, 4331−4342

microtubule surface after the recruitment of Src kinases by microtubule-associated proteins like tau. Finally, Dai et al. proposed that Cx43 and the MH2 region of Smad could compete for microtubule binding. On the basis of sequence similarities between Smad2-MH2 and K26D, we extracted the M19T peptide and showed that it effectively interacts with tubulin and MTs. Interestingly, this M19T peptide corresponds to amino acids located on the L3 loop of Smad2, which is required for phosphorylation and activation. Together, the K26D and M19T peptides delineate relevant binding sites that may be involved in the competition between Cx43 and Smad2-MH2 for tubulin and MT binding. This competition, however, may be based on more complex phenomena such as the contribution of an additional partner and the necessity to extend either K26D or M19T to introduce relevant contacts.

CONCLUSIONS

The results presented here show that a short peptide derived from the juxtamembrane region of Cx43 interacts specifically with tubulin and microtubules through a novel tubulin binding motif. Interestingly, the interaction of this peptide with tubulin and MTs is negatively regulated when the peptide is phosphorylated at a physiologically important location for gap-junctional communication. The structure data presented here will open the possibility of manipulating more precisely the interaction of Cx43 with the microtubule system to elucidate the multiple facets of Cx43 traffic and Cx43-dependent communication.

ASSOCIATED CONTENT

Supporting Information

Impact of K26D on in vitro microtubule assembly, K26D−BSA control interaction, and information about K26D−M19T competition for tubulin binding. This material is available free of charge via the Internet at http://pubs.acs.org.

Accession Codes

The atomic coordinates, chemical shifts, and NMR restraints have been deposited in the Protein Data Bank (entry 2LL2) and the BioMagResBank (entry 18022).

AUTHOR INFORMATION

Corresponding Author

*Phone: 33 1 69 47 01 87. Fax: 33 1 69 47 02 19. E-mail: pcurmi@univ-evry.fr (P.A.C.) or philippe.savarin@univ-paris13.fr (P.S.).

Present Address

[§]Université Abou Bekr Belkaid, Laboratoire de Recherche sur les Macromolécules (LRM), Tlemcen 13000, Algeria.

Funding

A.S.B.-N. is a recipient of a PNE fellowship from the Ministry of Higher Education and Scientific Research, Algeria. This work was supported in part by a French ANR (Agence nationale de la recherche) grant (ANR-08-JCJC-0081-01).

Notes

The authors declare no competing financial interest.

ACKNOWLEDGMENTS

We thank Universite Abou Bekr Belkaid (Tlemcen, Algeria) and Genopole (Evry, France) for continuous help. We thank Prof. Kenneth Downing (Bioenergy/GTL and Structural Biology Department, Lawrence Berkeley National Laboratory) for providing us with a reliable microtubule model used for the docking experiments.

ADDITIONAL NOTE

[a]In ref 12, a mistake appears in the numbering of amino acids of the juxtamembrane domain of Cx43, C260 being termed C263. A similar error appears in ref 13. We here use the Cx43 amino acid numbering as used in the Cx43 reference sequence for NCBI entry NP_000156.1.

REFERENCES

(1) Goodenough, D. A., Goliger, J. A., and Paul, D. L. (1996) Connexins, connexons, and intercellular communication. *Annu. Rev. Biochem. 65*, 475−502.

(2) Brissette, J. L., Kumar, N. M., Gilula, N. B., Hall, J. E., and Dotto, G. P. (1994) Switch in gap junction protein expression is associated with selective changes in junctional permeability during keratinocyte differentiation. *Proc. Natl. Acad. Sci. U.S.A. 91*, 6453−6457.

(3) Saez, J. C., Berthoud, V. M., Branes, M. C., Martinez, A. D., and Beyer, E. C. (2003) Plasma membrane channels formed by connexins: their regulation and functions. *Physiol. Rev. 83*, 1359−1400.

(4) Bodendiek, S. B., and Raman, G. (2010) Connexin modulators and their potential targets under the magnifying glass. *Curr. Med. Chem. 17*, 4191−4230.

(5) Sohl, G., and Willecke, K. (2004) Gap junctions and the connexin protein family. *Cardiovasc. Res. 62*, 228−232.

(6) Beyer, E. C., Paul, D. L., and Goodenough, D. A. (1987) Connexin43: A protein from rat heart homologous to a gap junction protein from liver. *J. Cell Biol. 105*, 2621−2629.

(7) Sosinsky, G. E., and Nicholson, B. J. (2005) Structural organization of gap junction channels. *Biochim. Biophys. Acta 1711*, 99−125.

(8) Haefliger, J. A., Bruzzone, R., Jenkins, N. A., Gilbert, D. J., Copeland, N. G., and Paul, D. L. (1992) Four novel members of the connexin family of gap junction proteins. Molecular cloning, expression, and chromosome mapping. *J. Biol. Chem. 267*, 2057−2064.

(9) Giepmans, B. N., and Moolenaar, W. H. (1998) The gap junction protein connexin43 interacts with the second PDZ domain of the zona occludens-1 protein. *Curr. Biol. 8*, 931−934.

(10) Giepmans, B. N. (2004) Gap junctions and connexin-interacting proteins. *Cardiovasc. Res. 62*, 233−245.

(11) Dbouk, H. A., Mroue, R. M., El Sabban, M. E., and Talhouk, R. S. (2009) Connexins: A myriad of functions extending beyond assembly of gap junction channels. *Cell Commun. Signaling 7*, 4.

(12) Giepmans, B. N., Verlaan, I., Hengeveld, T., Janssen, H., Calafat, J., Falk, M. M., and Moolenaar, W. H. (2001) Gap junction protein connexin-43 interacts directly with microtubules. *Curr. Biol. 11*, 1364−1368.

(13) Dai, P., Nakagami, T., Tanaka, H., Hitomi, T., and Takamatsu, T. (2007) Cx43 mediates TGF-β signaling through competitive Smads binding to microtubules. *Mol. Biol. Cell 18*, 2264−2273.

(14) Shaw, R. M., Fay, A. J., Puthenveedu, M. A., von Zastrow, M., Jan, Y. N., and Jan, L. Y. (2007) Microtubule plus-end-tracking proteins target gap junctions directly from the cell interior to adherens junctions. *Cell 128*, 547−560.

(15) Johnson, R. G., Meyer, R. A., Li, X. R., Preus, D. M., Tan, L., Grunenwald, H., Paulson, A. F., Laird, D. W., and Sheridan, J. D. (2002) Gap junctions assemble in the presence of cytoskeletal inhibitors, but enhanced assembly requires microtubules. *Exp. Cell Res. 275*, 67−80.

(16) Lauf, U., Giepmans, B. N., Lopez, P., Braconnot, S., Chen, S. C., and Falk, M. M. (2002) Dynamic trafficking and delivery of connexons to the plasma membrane and accretion to gap junctions in living cells. *Proc. Natl. Acad. Sci. U.S.A. 99*, 10446−10451.

(17) Paulson, A. F., Lampe, P. D., Meyer, R. A., TenBroek, E., Atkinson, M. M., Walseth, T. F., and Johnson, R. G. (2000) Cyclic AMP and LDL trigger a rapid enhancement in gap junction assembly

through a stimulation of connexin trafficking. *J. Cell Sci. 113* (Part 17), 3037−3049.
(18) Martin, P. E., Blundell, G., Ahmad, S., Errington, R. J., and Evans, W. H. (2001) Multiple pathways in the trafficking and assembly of connexin 26, 32 and 43 into gap junction intercellular communication channels. *J. Cell Sci. 114*, 3845−3855.
(19) Lampe, P. D., TenBroek, E. M., Burt, J. M., Kurata, W. E., Johnson, R. G., and Lau, A. F. (2000) Phosphorylation of connexin43 on serine368 by protein kinase C regulates gap junctional communication. *J. Cell Biol. 149*, 1503−1512.
(20) Solan, J. L., and Lampe, P. D. (2009) Connexin43 phosphorylation: Structural changes and biological effects. *Biochem. J. 419*, 261−272.
(21) Kanemitsu, M. Y., and Lau, A. F. (1993) Epidermal growth factor stimulates the disruption of gap junctional communication and connexin43 phosphorylation independent of 12-0-tetradecanoylphorbol 13-acetate-sensitive protein kinase C: The possible involvement of mitogen-activated protein kinase. *Mol. Biol. Cell 4*, 837−848.
(22) Warn-Cramer, B. J., Lampe, P. D., Kurata, W. E., Kanemitsu, M. Y., Loo, L. W., Eckhart, W., and Lau, A. F. (1996) Characterization of the mitogen-activated protein kinase phosphorylation sites on the connexin-43 gap junction protein. *J. Biol. Chem. 271*, 3779−3786.
(23) Le, A. C., and Musil, L. S. (2001) A novel role for FGF and extracellular signal-regulated kinase in gap junction-mediated intercellular communication in the lens. *J. Cell Biol. 154*, 197−216.
(24) Polontchouk, L., Ebelt, B., Jackels, M., and Dhein, S. (2002) Chronic effects of endothelin 1 and angiotensin II on gap junctions and intercellular communication in cardiac cells. *FASEB J. 16*, 87−89.
(25) Dong, C., Li, Z., Alvarez, R., Jr., Feng, X. H., and Goldschmidt-Clermont, P. J. (2000) Microtubule binding to Smads may regulate TGF β activity. *Mol. Cell 5*, 27−34.
(26) Zhu, S., Goldschmidt-Clermont, P. J., and Dong, C. (2004) Transforming growth factor-β-induced inhibition of myogenesis is mediated through Smad pathway and is modulated by microtubule dynamic stability. *Circ. Res. 94*, 617−625.
(27) Castoldi, M., and Popov, A. V. (2003) Purification of brain tubulin through two cycles of polymerization-depolymerization in a high-molarity buffer. *Protein Expression Purif. 32*, 83−88.
(28) Detrich, H. W., III, and Williams, R. C. (1978) Reversible dissociation of the $\alpha\beta$ dimer of tubulin from bovine brain. *Biochemistry 17*, 3900−3917.
(29) Johnson, B. A., and Blevins, R. A. (1994) NMRView: A Computer Program for the Visualization and Analysis of NMR Data. *J. Biomol. NMR 4*, 603−614.
(30) Hwang, T. L., and Shaka, A. J. (1995) Water Suppression That Works. Excitation Sculpting Using Arbitrary Wave-Forms and Pulsed-Field Gradients. *J. Magon. Reson., Ser. A 112*, 275−279.
(31) Piotto, M., Saudek, V., and Sklenar, V. (1992) Gradient-tailored excitation for single-quantum NMR spectroscopy of aqueous solutions. *J. Biomol. NMR 2*, 661−665.
(32) Wüthrich, K. (1986) *NMR of Proteins and Nucleic Acids*, John Wiley & Sons, New York.
(33) Braunschweiler, L., and Ernst, R. R. (1983) Coherence transfer by isotropic mixing: Application to proton correlation spectroscopy. *J. Magn. Reson. 53*, 521−528.
(34) Kumar, A., Ernst, R. R., and Wüthrich, K. (1980) A two-dimensional nuclear Overhauser enhancement (2D NOE) experiment for the elucidation of complete proton-proton cross-relaxation networks in biological macromolecules. *Biochem. Biophys. Res. Commun. 95*, 1−6.
(35) Clore, G. M., and Gronenborn, A. M. (1982) Theory and applications of the transferred nuclear Overhauser effect to the study of the conformations of small ligands bound to proteins. *J. Magn. Reson. 48*, 402−417.
(36) Clore, G. M., and Gronenborn, A. M. (1983) Theory of the time dependent transferred nuclear Overhauser effect: Application to the structural analysis of ligand-protein complexes in solution. *J. Magn. Reson. 53*, 423−442.
(37) Mayer, M., and Meyer, B. (1999) Characterization of Ligand Binding by Saturation Transfer Difference NMR Spectra. *Angew. Chem., Int. Ed. 35*, 1784−1788.
(38) Brunger, A. T., Adams, P. D., Clore, G. M., DeLano, W. L., Gros, P., Grosse-Kunstleve, R. W., Jiang, J. S., Kuszewski, J., Nilges, M., Pannu, N. S., Read, R. J., Rice, L. M., Simonson, T., and Warren, G. L. (1998) Crystallography & NMR system: A new software suite for macromolecular structure determination. *Acta Crystallogr. D54* (Part 5), 905−921.
(39) Cornilescu, G., Delaglio, F., and Bax, A. (1999) Protein backbone angle restraints from searching a database for chemical shift and sequence homology. *J. Biomol. NMR 13*, 289−302.
(40) Baleja, J., Moult, J., and Sykes, B. D. (1990) Distance measurement and structure refinement with NOE data. *J. Magn. Reson. 87*, 375−384.
(41) Laskowski, R. A., MacArthur, M. W., Moss, D. A., and Thornton, J. M. (1993) PROCHECK: A program to check the stereochemical quality of protein structures. *J. Appl. Crystallogr. 26*, 283−291.
(42) Koradi, R., Billeter, M., and Wuthrich, K. (1996) MOLMOL: A program for display and analysis of macromolecular structures. *J. Mol. Graphics 14*, 51−32.
(43) Basdevant, N., Borgis, D., and Ha-Duong, T. (2007) A coarse-grained protein-protein potential derived from an all-atom force field. *J. Phys. Chem. B 111*, 9390−9399.
(44) Zacharias, M. (2005) ATTRACT: Protein-protein docking in CAPRI using a reduced protein model. *Proteins 60*, 252−256.
(45) Clement, M. J., Kuoch, B. T., Ha-Duong, T., Joshi, V., Hamon, L., Toma, F., Curmi, P. A., and Savarin, P. (2009) The stathmin-derived I19L peptide interacts with FtsZ and alters its bundling. *Biochemistry 48*, 9734−9744.
(46) *The PyMOL Molecular Graphics System*, version 1.3 (2011) Schrodinger, LLC, New York.
(47) Chernov, K. G., Mechulam, A., Popova, N. V., Pastre, D., Nadezhdina, E. S., Skabkina, O. V., Shanina, N. A., Vasiliev, V. D., Tarrade, A., Melki, J., Joshi, V., Baconnais, S., Toma, F., Ovchinnikov, L. P., and Curmi, P. A. (2008) YB-1 promotes microtubule assembly in vitro through interaction with tubulin and microtubules. *BMC Biochem. 9*, 23.
(48) Clement, M. J., Savarin, P., Adjadj, E., Sobel, A., Toma, F., and Curmi, P. A. (2010) Probing interactions of tubulin with small molecules, peptides, and protein fragments by solution nuclear magnetic resonance. *Methods Cell Biol. 95*, 407−447.
(49) Clement, M. J., Jourdain, I., Lachkar, S., Savarin, P., Gigant, B., Knossow, M., Toma, F., Sobel, A., and Curmi, P. A. (2005) N-Terminal stathmin-like peptides bind tubulin and impede microtubule assembly. *Biochemistry 44*, 14616−14625.
(50) Clement, M. J., Kuoch, B. T., Ha-Duong, T., Joshi, V., Hamon, L., Toma, F., Curmi, P. A., and Savarin, P. (2009) The stathmin-derived I19L peptide interacts with FtsZ and alters its bundling. *Biochemistry 48*, 9734−9744.
(51) Söding, J. (2005) Protein homology detection by HMM-HMM comparison. *Bioinformatics 21*, 951−960.
(52) Wishart, D. S., and Sykes, B. D. (1994) The ^{13}C chemical-shift index: A simple method for the identification of protein secondary structure using ^{13}C chemical-shift data. *J. Biomol. NMR 4*, 171−180.
(53) Shen, Y., Delaglio, F., Cornilescu, G., and Bax, A. (2009) TALOS+: A hybrid method for predicting protein backbone torsion angles from NMR chemical shifts. *J. Biomol. NMR 44*, 213−223.
(54) Lin, R., Warn-Cramer, B. J., Kurata, W. E., and Lau, A. F. (2001) v-Src phosphorylation of connexin 43 on Tyr247 and Tyr265 disrupts gap junctional communication. *J. Cell Biol. 154*, 815−827.
(55) Lin, R., Martyn, K. D., Guyette, C. V., Lau, A. F., and Warn-Cramer, B. J. (2006) v-Src tyrosine phosphorylation of connexin43: Regulation of gap junction communication and effects on cell transformation. *Cell Commun. Adhes. 13*, 199−216.
(56) Wu, J. W., Hu, M., Chai, J., Seoane, J., Huse, M., Li, C., Rigotti, D. J., Kyin, S., Muir, T. W., Fairman, R., Massague, J., and Shi, Y. (2001) Crystal structure of a phosphorylated Smad2. Recognition of

phosphoserine by the MH2 domain and insights on Smad function in TGF-β signaling. *Mol. Cell 8*, 1277−1289.
(57) Sanchez-Pedregal, V. M., Reese, M., Meiler, J., Blommers, M. J., Griesinger, C., and Carlomagno, T. (2005) The INPHARMA method: Protein-mediated interligand NOEs for pharmacophore mapping. *Angew. Chem., Int. Ed. 44*, 4172−4175.
(58) Becattini, B., and Pellecchia, M. (2006) SAR by ILOEs: An NMR-based approach to reverse chemical genetics. *Chemistry 12*, 2658−2662.
(59) Ravelli, R. B. G., Gigant, B., Curmi, P. A., Jourdain, I., Lachkar, S., Sobel, A., and Knossow, M. (2004) Insight into tubulin regulation from a complex with colchicine and a stathmin-like domain. *Nature 428*, 198−202.
(60) Crow, D. S., Beyer, E. C., Paul, D. L., Kobe, S. S., and Lau, A. F. (1990) Phosphorylation of connexin43 gap junction protein in uninfected and Rous sarcoma virus-transformed mammalian fibroblasts. *Mol. Cell. Biol. 10*, 1754−1763.
(61) Toyofuku, T., Yabuki, M., Otsu, K., Kuzuya, T., Hori, M., and Tada, M. (1998) Direct association of the gap junction protein connexin-43 with ZO-1 in cardiac myocytes. *J. Biol. Chem. 273*, 12725−12731.
(62) Thomas, T., Jordan, K., and Laird, D. W. (2001) Role of cytoskeletal elements in the recruitment of Cx43-GFP and Cx26-YFP into gap junctions. *Cell Commun. Adhes. 8*, 231−236.
(63) Francis, R., Xu, X., Park, H., Wei, C. J., Chang, S., Chatterjee, B., and Lo, C. (2011) Connexin43 modulates cell polarity and directional cell migration by regulating microtubule dynamics. *PLoS One 6*, e26379.
(64) Shen, V., Rifas, L., Kohler, G., and Peck, W. A. (1986) Prostaglandins change cell shape and increase intercellular gap junctions in osteoblasts cultured from rat fetal calvaria. *J. Bone Miner. Res. 1*, 243−249.
(65) Guo, Y., Martinez-Williams, C., and Rannels, D. E. (2003) Gap junction-microtubule associations in rat alveolar epithelial cells. *Am. J. Physiol. 285*, L1213−L1221.